THE EFFECT OF DISPERSOIDS ON FATIGUE CRACK PROPAGATION IN Al-Zn-Mg ALLOYS

M. Harrison* and J.W. Martin**

The effects of Mn-bearing and of Zr-bearing dispersoids upon FCG were studied in peak-aged alloys of similar grain sizes and comparable yield stresses. da/dN vs. ΔK curves were measured in the threshold range, at R-values of 0.1 and 0.7.

The presence of a high volume fraction of the Mn-bearing dispersoids lowered the threshold ΔK. It is proposed that the homogenization of dislocation distribution reduces the tendency for slip reversibility. The Zr-bearing dispersoids do not homogenise slip, and their effect is to raise the ΔK threshold without changing the (predominantly intergranular) fracture mode. It is suggested that their action is to reduce hydrogen embrittlement.

INTRODUCTION

Commercial heat-treatable aluminium alloys contain dispersoids, which are fine particles of intermetallic phases arising from the addition of a transition element such as Cr, Mn, Zr or V. Their prime function is to control grain growth during heat-treatment. However, under conditions of monotonic straining, Cr- and Mn-bearing dispersoids have been shown to promote homogenization of slip (1,2) which, together with the refined grain size, increases the tensile ductility and also the fracture toughness (3,4). Edwards and Martin have also shown that the addition of Mn-bearing dispersoids to peak-aged Al-Mg-Si alloys can result in improved properties with regard to the initiation and propagation of fatigue cracks under high cycle (5) and low cycle (6) conditions.

Little systematic work has been carried out in this area on the medium-strength Al-Zn-Mg alloys, and the object of the present work has been to compare the effects upon fatigue crack

* Risley Nuclear Power Development Labs, UKAEA, Warrington
** Dept. of Metallurgy & Science of Materials, Oxford University

propagation of Mn-bearing and Zr-bearing dispersoids. The former consist of a uniform dispersion of non-coherent particles of intermetallic phase; the latter are distributed as clusters of coherent particles. A ternary (dispersoid-free) alloy was studied for comparative purposes.

EXPERIMENTAL

The alloys were prepared from high purity (low Fe) material in order to minimize the occurrence of coarse residual particles, whose effect might be to swamp that of the dispersoids themselves. The composition of the alloys is given in Table 1.

TABLE 1 - Composition of the alloys.

Alloy	wt% Cu	Fe	Mg	Mn	Si	Ti	Zn	Zr
CT	0.01	0.004	1.71	0.001	0.004	0.001	5.43	-
CML	0.01	0.006	1.73	0.22	0.04	0.001	5.58	-
CMH	0.001	0.007	1.66	0.42	0.08	0.001	5.47	-
CZL	0.001	0.007	1.67	0.003	0.006	0.001	5.37	0.08
CZH	0.001	0.01	1.64	0.004	0.01	0.001	5.37	0.15

All the alloys were subjected to thermo-mechanical treatments such that the grain structures were equiaxed and recrystallized. They were given a common solution-treatment at 475°C, followed by water quenching and 24 hr ageing at room temperature. The alloys were then artificially aged at 130°C for 60 hr, which corresponded to peak hardness. The yield stresses obtained from the average of several tensile tests, and the grain sizes of the alloys are given in Table 2.

TABLE 2 - Grain sizes, dispersoid sizes and Yield Stresses

Alloy	Grain Size (μm)	Dispersoid Size (μm)	Yield Stress (MPa)
CT	105	-	408
CML	108	0.1	412
CMH	101	0.1	399
CZL	105	0.02	380
CZH	80	0.04	355

Each alloy had similar dispersions of the ageing precipitate, both within the grains and at grain boundaries. The particle-size of the dispersoids is given in Table 2, and figs. 1 and 2 show their distributions in CMH and CZH respectively. In CML the dispersoid distribution is very sparse - the precipitates are observed to be primarily at sites corresponding to grain boundaries in the as-cast structure. The dispersoid distribution in CZL appeared similar to that in CZH.

Fatigue crack propagation tests were conducted on a servohydraulic machine operating in closed loop configuration under load control. Tests were performed on CT specimens of 6 mm thickness in laboratory air (RH approximately 60%) at constant stress intensity. Load-shedding was controlled by a microcomputer interfaced to the fatigue machine. Crack length was monitored by a DC potential drop technique.

Log. crack growth rate (da/dN) verses stress intensity range (ΔK) curves were plotted for alloys CT, CML, CZL and CZH at R-values of 0.1, and for all five of the alloys at an R-value of 0.7. This has enabled the effects of the dispersoids upon the fatigue thresholds to be identified.

EXPERIMENTAL RESULTS

Figs. 3 and 4 show the crack propagation behaviour of the alloys at R-values of 0.1 and 0.7 respectively. It can be seen that the data obtained at the higher R-value are shifted to lower values of ΔK, in comparison with those obtained at R = 0.1. This confirms the presence of crack closure in the experiments at R = 0.1, and it is likely that this effect is minimised in the R = 0.7 experiments.

The most important factor in the present context is that the sequence of the threshold data points for the alloys is similar in figs. 3 and 4. This indicates that there is also present an effect upon the value of the ΔK thresholds arising from the differences in microstructure, and which are independent of the degree of crack closure.

In fig 4, the data points fall into three groups, in the first of which the highest crack propagation rate, and the lowest ΔK threshold is observed in alloy CMH, which contains a high volume fraction of the Mn-bearing dispersoids. In the second group of data. the dispersoid-free alloy (CT) and low-manganese materials (CML) behave similarly, and exhibit the next highest ΔK threshold value, and the next lower crack propagation rate.

The third group of data points are those due to specimens containing the zirconium-bearing dispersoids, CZL and CZH. These specimens exhibit the highest ΔK threshold values, and the minimum crack propagation rates at a given ΔK.

In each of the above cases, the crack propagation paths have been studied by SEM examination of the fracture surfaces. For all except the CMH material, the fracture surfaces were characterised by a high percentage (approximately 80%) of intergranular failure, which varied little from alloy to alloy. The specimens tested at R = 0.1 tended to show evidence of wear debris, doubtless due to crack closure effects during the test (e.g. fig.5, which also shows many smooth, featureless grain boundary surfaces).

The intergranular facets on the zirconium-containing material were significantly different, however. Although the overall proportion of intergranular failure was similar to that in CT (and CML), the grain boundary facets showed evidence of (a) local microvoid coalescence by ductile dimple formation, (fig.6) and (b) local circular pores associated with dispersoid particles (fig 7).

In the case of the high-manganese alloy, the fracture surfaces exhibited significantly less intergranular character (approximately 20 - 30%), and again (fig.8) some evidence of porosity associated with the dispersoid phase.

DISCUSSION

The essential difference between the alloys in the present work is that of slip distribution arising from the differences in the dispersoid phases present. Grain sizes and yield stresses are comparable in all cases, but the manganese-bearing and zirconium-bearing dispersoids are likely to give rise to different effects. The Mn-dispersoids are well known (2) to have the effect of slip homogenisation to a degree depending upon the volume fraction present, whereas the Zr-dispersoids are coherent and are unlikely to homogenise slip.

The behaviour of CMH in fig.4 is thus readily interpreted, if it is assumed that the high volume fraction of Mn-dispersoids present have increased the homogeneity of slip. This will have two effects, firstly the proportion of intergranular fracture will decrease, due to the reduction of grain boundary stress concentrations associated with slip bands, and secondly the resulting lack of strain reversibility will lower the ΔK threshold, as proposed by Hornbogen and Zum Gahr (7).

The absence of any effect in the low Mn-alloy (CML) is presumably from the inadequate volume fraction of the dispersoid phase present to influence the slip distribution in any way.

The evident beneficial effect of the Zr-dispersoids is unlikely to arise from change in slip distribution due to the presence of this phase. The dispersoids are in the form of coherent particles, and these will presumably be sheared in the same way as the ageing precipitate and thus have no slip-homogenising effect. This is supported from the absence of any change from CT in the proportion of intergranular fracture observed in CZM and CZL.

The intergranular fracture surfaces are however changed in the Zr-bearing alloys, in that (a) the surfaces are no longer smooth and featureless, but show a slight evidence of local ductile cusp formation (fig 6), and (b) porosity is observed to be associated with dispersoids on the fracture surface (fig.7). These observations are consistent with the dispersoids influencing the degree of hydrogen embrittlement in the material.

Al-Zn-Mg alloys become embrittled during exposure to moist environments due to hydrogen penetration of grain boundaries. This is characterised by the coincidence of the fracture path with the grain boundary plane, and the wholly brittle nature of the intergranular fracture at the highest resolutions studied.

Scamans (8) has reported that certain particles of incoherent phases present on the grain boundary may promote the formation of hydrogen bubbles, thus locally decreasing the embrittlement of the grain boundary plane itself. Scamans reports that the intermetallic particles present in his alloys due to the addition of transition elements showed a distinct propensity to act in this way, and he gave evidence of Mn-rich phases being associated with grain boundary hydrogen bubbles. It is proposed that the Zr-rich particles may be acting as local hydrogen getters in the present CZL and CZH alloys, and that the voids evident on the fracture surface (fig.7) are in fact such hydrogen bubbles.

The reason why the effect is not observed in the CMH is that the (unsheared) particles of Mn-bearing dispersoid have homogenised the slip, thus reducing the stresses on the grain boundaries and thus reducing the propensity for intergranular fracture.

CONCLUSIONS

1. A high volume fraction of incoherent particles of Mn-bearing dispersoid lowers the threshold ΔK compared with the dispersoid-free material, and decreases the proportion of intergranular fracture . This is due to the slip-homogenizing effect of this dispersoid which reduces both the reversibility of the slip and also the strain concentrations where slip bands meet the grain boundaries.

2. The coherent particles of Zr-bearing dispersoids do not have a slip-homogenizing effect and thus do not change the proportion of intergranular fracture. Their presence raises the ΔK threshold, possibly through operating as hydrogen getters, thus increasing the work of grain boundary fracture.

ACKNOWLEDGEMENTS

The authors are grateful to Professor Sir Peter Hirsch, FRS, for laboratory facilities, , and to the SERC and Messrs Alcan International Limited for financial and material support.

REFERENCES

(1) Lutjering, G., Doker, H., and Munz, D., Proc. 3rd Int. Conf. on Strength of Metals and Alloys (Cambridge), The Institute of Metals, Vol.1, 1973,pp 427-431.

(2) Dowling, J.M. and Martin, J.W., Acta Met., Vol. 24, 1976, pp 1147-1153.

(3) Prince, K.C. and Martin, J.W., Acta Met., Vol. 27, 1979, pp 1401- 1408.

(4) Blind, J.A. and Martin, J.W., Mat. Sci.Eng., Vol.57, 1983, pp 49-54.

(5) Edwards, L., and Martin, J.W., Metal Science, Vol. 17, 1983, pp 511-518.

(6) Edwards, L., and Martin, J.W., 6th Int. Conf. on Strength of Metals and Alloys (Melbourne), 1982, p.873.

(7) Hornbogen, E., and Zum Gahr, K.H., Acta Met., Vol. 24 1976, pp 581 - 592.

(8) Scamans, G.M., J. Mat. Sci., Vol. 13, 1978, pp 27-36.

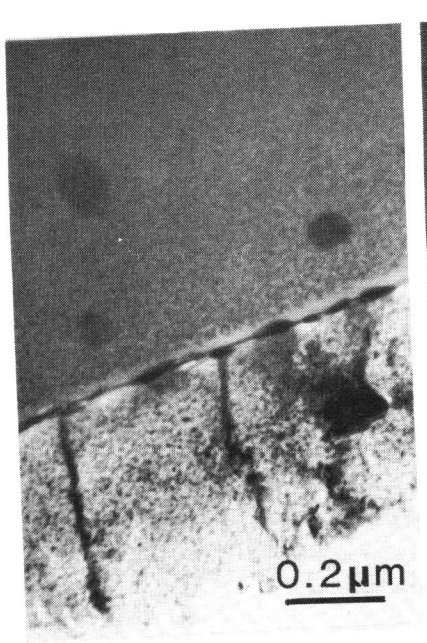

Fig.1. TEM of alloy CMH

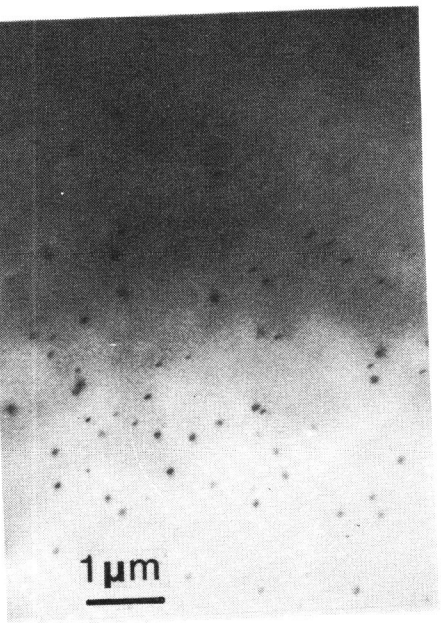

Fig.2. TEM of alloy CZH

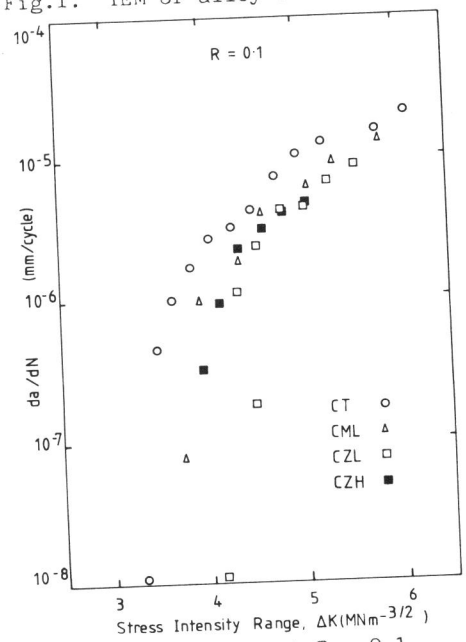

Fig.3. FCGR data at R = 0.1

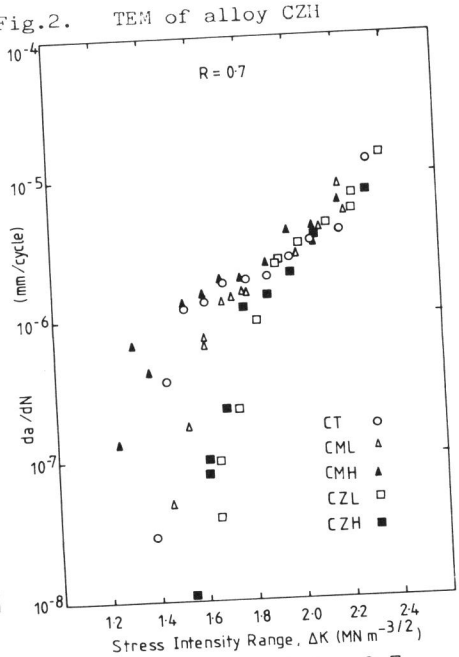

Fig.4. FCGR data at R = 0.7

Fig.5. SEM of fracture surface of alloy CT (R = 0.1).

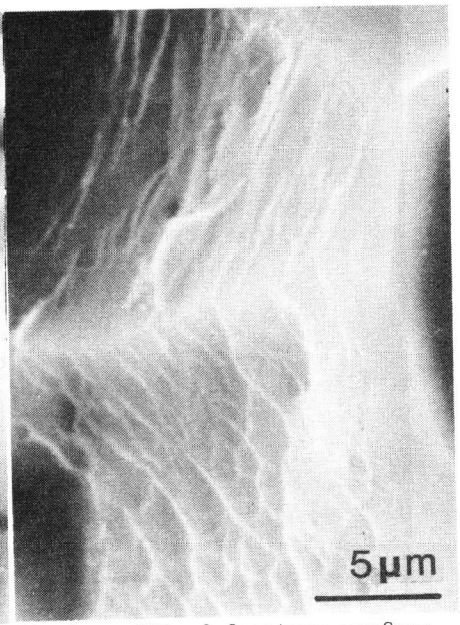

Fig.6. SEM of fracture surface of alloy CZL (R = 0.7).

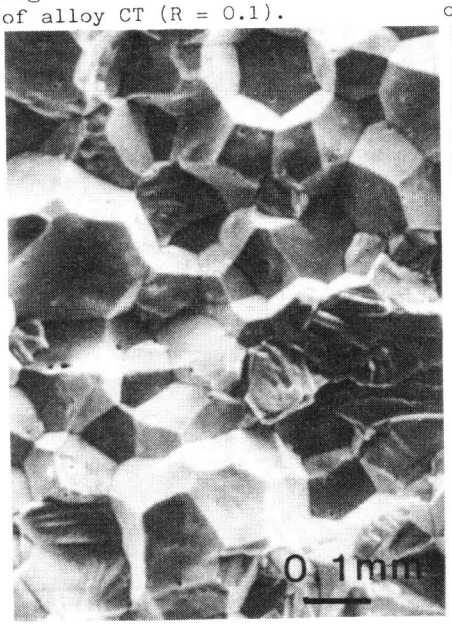

Fig.7. SEM of fracture surface of alloy CZH (R = 0.7).

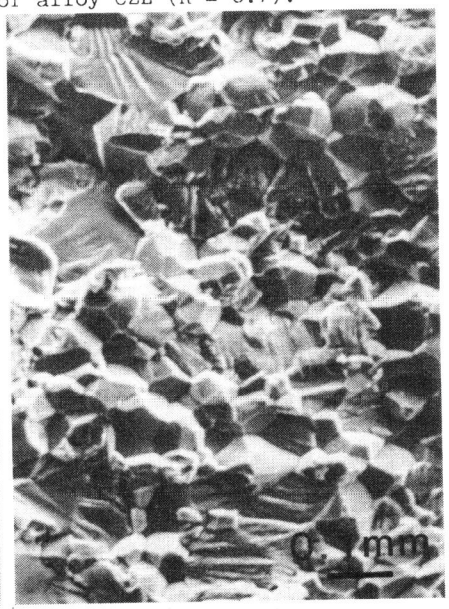

Fig.8. SEM of fracture surface of alloy CMH (R = 0.7).